

## Bis( $\beta$ -diketone)-based metallacycles with Haloalkane-induced Fluorescence Enhancement

*Ming-Jie Yan, Tian-Fu Liu,\* Sheng-Li Huang\* and Guo-Yu Yang\**

School of Chemistry and Chemical Engineering, Beijing Institute of Technology,  
Beijing 100081, China

### 1. Materials and methods

The ligand **1**, 4-bis-(3'-acetylacetonate)benzene ( $H_2L_1$ ) and **4**, 4'-bis-(3'-acetylacetonate)biphenylene ( $H_2L_2$ ) were prepared by the literature method.<sup>1</sup> All other reagents were commercially available and used as received. The  $^1H$ ,  $^{13}C\{^1H\}$  NMR spectra were recorded on a Bruker Avance III HD 400 spectrometer using the residual protonated solvent as internal standard. Infrared spectra were recorded as KBr pellets on Thermo Fisher Scientific FT-IR spectrometer (Thermo IS5). The photoluminescence (PL) excitation and emission spectra were performed on a Hitachi F-7000 spectrophotometer equipped with a 150W xenon lamp as the excitation source at room temperature. ESI-MS spectra were recorded on Agilent Q-TOF 6520 mass spectrometer.

### 2. Synthesis of 1-5

**Synthesis of Metallarectangles 1-3:** A mixture of  $[Ru_2(p\text{-cymene})_2Cl_4]$  (0.05 mmol) and one equivalent of NNN ligand (0.05 mmol) in dichloromethane (4 mL) was stirred for 24 h, then added four equivalents of  $AgPF_6$  (0.20 mmol) and one equivalent of  $H_2L_1$  (0.05 mmol) the corresponding in this solution and kept stirring for 24 h, finally filtered to remove  $AgCl$ . The solvent was removed under vacuum and the residue was taken up in dichloromethane (2 mL) and diethyl ether was added to precipitate the product as yellow solids **1-3**.

**1:** Yield 65 mg, (88%). FT-IR spectrum (KBr,  $\nu$ ,  $cm^{-1}$ ):  $\nu = 3429$  (s), 2975 (w), 1581 (s), 1415 (m), 1342 (m), 1286 (w), 1046(m), 842 (s), 732 (w), 622 (w), 566 (w)  $cm^{-1}$ .  $^1H$ -NMR (400 MHz,  $DMSO-d_6$ ):  $\delta = 8.66$  (d,  $^3J_{H,H} = 4$  Hz, 8 H,  $H_{bpy}$ ), 8.21 (d,  $^3J_{H,H} = 4$  Hz, 8 H,  $H_{bpy}$ ), 7.13 (s, 4 H,  $H_{Ar}$ ), 6.26 (s, 4 H,  $H_{Ar}$ ), 5.98 (d,  $^3J_{H,H} = 8$  Hz, 8 H,  $H_{cymene}$ ), 5.74 (d,  $^3J_{H,H} = 4$  Hz, 8 H,  $H_{cymene}$ ), 2.05 [s, 12H,  $ArCH_3$ ], 1.65 (s, 24 H,  $L-CH_3$ ), 1.33 [d,  $^3J_{H,H} = 8$  Hz, 24H,  $CH(CH_3)_2$ ] ppm.  $^{13}C$ -NMR (400 MHz,  $DMSO-d_6$ ):  $\delta = 186.62$  (CO), 153.49 ( $CH_{bpy}$ ), 144.93 ( $C_{bpy}$ ), 138.88 ( $C_{L1}$ ), 132.55 ( $C_{L1}$ ), 131.99 ( $C_{L1}$ ), 123.68 ( $CH_{bpy}$ ), 113.77 ( $C_{L1}$ ), 102.20 ( $C_{cymene}$ ), 99.42 ( $C_{cymene}$ ), 85.11 ( $CH_{cymene}$ ), 81.72 ( $CH_{cymene}$ ), 30.74 ( $ArCH_3$ ), 27.91 ( $L-CH_3$ ), 22.39 [ $CH(CH_3)_2$ ], 17.24 [ $CH(CH_3)_2$ ] ppm.

**2:** Yield 72 mg, (93%). FT-IR spectrum (KBr,  $\nu$ ,  $\text{cm}^{-1}$ ):  $\nu = 2982$  (w), 1565 (s), 1431 (m), 1343 (m), 1285 (w), 1092(m), 1035(w), 975 (s), 841 (s), 724 (w), 547 (w), 487 (w)  $\text{cm}^{-1}$ .  $^1\text{H-NMR}$  (400 MHz,  $\text{DMSO-d}_6$ ):  $\delta = 8.54$  (d,  $^3J_{\text{H,H}} = 4$  Hz, 8 H,  $\text{H}_{\text{bpb}}$ ), 8.14 (s, 8 H,  $\text{H}_{\text{bpb}}$ ), 8.11 (d,  $^3J_{\text{H,H}} = 8$  Hz, 8 H,  $\text{H}_{\text{bpb}}$ ), 7.15 (s, 4 H,  $\text{H}_{\text{Ar}}$ ), 6.30 (s, 4 H,  $\text{H}_{\text{Ar}}$ ), 5.97 (d,  $^3J_{\text{H,H}} = 8$  Hz, 8 H,  $\text{H}_{\text{cymene}}$ ), 5.74 (d,  $^3J_{\text{H,H}} = 8$  Hz, 8 H,  $\text{H}_{\text{cymene}}$ ), 2.07 [s, 12H,  $\text{ArCH}_3$ ], 1.69 (s, 24 H, L- $\text{CH}_3$ ), 1.33 [d,  $^3J_{\text{H,H}} = 4$  Hz, 24H,  $\text{CH}(\text{CH}_3)_2$ ] ppm.  $^{13}\text{C-NMR}$  (400 MHz,  $\text{DMSO-d}_6$ ):  $\delta = 186.70$  (CO), 153.11 ( $\text{CH}_{\text{bpb}}$ ), 148.46 ( $\text{C}_{\text{bpb}}$ ), 138.73 ( $\text{C}_{\text{L1}}$ ), 137.40 ( $\text{C}_{\text{bpb}}$ ), 132.73 ( $\text{C}_{\text{L1}}$ ), 132.05 ( $\text{C}_{\text{L1}}$ ), 128.66 ( $\text{CH}_{\text{bpb}}$ ), 123.63 ( $\text{CH}_{\text{bpb}}$ ), 113.61 ( $\text{C}_{\text{L1}}$ ), 102.17 ( $\text{C}_{\text{cymene}}$ ), 99.14 ( $\text{C}_{\text{cymene}}$ ), 84.69 ( $\text{CH}_{\text{cymene}}$ ), 81.68 ( $\text{CH}_{\text{cymene}}$ ), 30.74 ( $\text{ArCH}_3$ ), 27.99 (L- $\text{CH}_3$ ), 22.66 [ $\text{CH}(\text{CH}_3)_2$ ], 17.26 [ $\text{CH}(\text{CH}_3)_2$ ] ppm.

**3:** Yield 62 mg, (85%). FT-IR spectrum (KBr,  $\nu$ ,  $\text{cm}^{-1}$ ):  $\nu = 3655$  (w), 2968 (w), 1565 (s), 1417 (m), 1343 (m), 1035(m), 841 (s), 636 (w), 561 (w), 459 (w)  $\text{cm}^{-1}$ .  $^1\text{H-NMR}$  (400 MHz,  $\text{DMSO-d}_6$ ):  $\delta = 8.50$  (d,  $^3J_{\text{H,H}} = 8$  Hz, 8 H,  $\text{H}_{\text{bpd}}$ ), 8.03 (d,  $^3J_{\text{H,H}} = 4$  Hz, 16 H,  $\text{H}_{\text{bpd}}$ ), 7.94 (d,  $^3J_{\text{H,H}} = 12$  Hz, 8 H,  $\text{H}_{\text{bpd}}$ ), 7.15 (s, 4 H,  $\text{H}_{\text{Ar}}$ ), 6.07 (s, 4 H,  $\text{H}_{\text{Ar}}$ ), 5.97 (d,  $^3J_{\text{H,H}} = 8$  Hz, 8 H,  $\text{H}_{\text{cymene}}$ ), 5.75 (d,  $^3J_{\text{H,H}} = 8$  Hz, 8 H,  $\text{H}_{\text{cymene}}$ ), 2.11 [s, 12H,  $\text{ArCH}_3$ ], 1.68 (s, 24 H, L- $\text{CH}_3$ ), 1.34 [d,  $^3J_{\text{H,H}} = 4$  Hz, 24H,  $\text{CH}(\text{CH}_3)_2$ ] ppm.  $^{13}\text{C-NMR}$  (400 MHz,  $\text{DMSO-d}_6$ ):  $\delta = 186.39$  (CO), 152.93 ( $\text{CH}_{\text{bpd}}$ ), 149.20 ( $\text{C}_{\text{bpd}}$ ), 141.29 ( $\text{C}_{\text{bpd}}$ ), 138.79 ( $\text{C}_{\text{L1}}$ ), 135.26 ( $\text{C}_{\text{bpd}}$ ), 132.48 ( $\text{C}_{\text{L1}}$ ), 131.46 ( $\text{C}_{\text{L1}}$ ), 128.32 ( $\text{CH}_{\text{bpd}}$ ), 126.63 ( $\text{CH}_{\text{bpd}}$ ), 123.33 ( $\text{CH}_{\text{bpd}}$ ), 113.96 ( $\text{C}_{\text{L1}}$ ), 102.05 ( $\text{C}_{\text{cymene}}$ ), 99.04 ( $\text{C}_{\text{cymene}}$ ), 84.60 ( $\text{CH}_{\text{cymene}}$ ), 82.09 ( $\text{CH}_{\text{cymene}}$ ), 30.77 ( $\text{ArCH}_3$ ), 27.96 (L- $\text{CH}_3$ ), 22.40 [ $\text{CH}(\text{CH}_3)_2$ ], 17.56 [ $\text{CH}(\text{CH}_3)_2$ ] ppm.

Synthesis of Metalla-Rectangles **4** and **5**: these rectangles were synthesized in a procedure analogous to that of **1-3** except that  $\text{H}_2\text{L}_1$  was took the place of  $\text{H}_2\text{L}_2$  (0.05 mmol). The yellow solids were obtained.

**4:** Yield 69 mg, (90%). FT-IR spectrum (KBr,  $\nu$ ,  $\text{cm}^{-1}$ ):  $\nu = 3646$  (s), 2969 (w), 2356 (w), 1609 (w), 1569 (s), 1415 (m), 1353 (m), 1306 (w), 1266 (m), 1112 (m), 1058 (s), 829 (s), 748 (s), 634 (w), 486 (m)  $\text{cm}^{-1}$ .  $^1\text{H-NMR}$  (400 MHz,  $\text{DMSO-d}_6$ ):  $\delta = 8.71$  (d,  $^3J_{\text{H,H}} = 8$  Hz, 8 H,  $\text{H}_{\text{bpy}}$ ), 8.16 (d,  $^3J_{\text{H,H}} = 8$  Hz, 8 H,  $\text{H}_{\text{bpy}}$ ), 6.90 (s, 8 H,  $\text{H}_{\text{Ar}}$ ), 6.35 (d,  $^3J_{\text{H,H}} = 4$  Hz, 4 H,  $\text{H}_{\text{Ar}}$ ), 6.04 (d,  $^3J_{\text{H,H}} = 8$  Hz, 8 H,  $\text{H}_{\text{cymene}}$ ), 5.82 (d,  $^3J_{\text{H,H}} = 8$  Hz, 8 H,  $\text{H}_{\text{cymene}}$ ), 5.36 (d,  $^3J_{\text{H,H}} = 8$  Hz, 4 H,  $\text{H}_{\text{Ar}}$ ), 2.20 [s, 12H,  $\text{ArCH}_3$ ], 1.60 (s, 24 H, L- $\text{CH}_3$ ), 1.38 [d,  $^3J_{\text{H,H}} = 4$  Hz, 24H,  $\text{CH}(\text{CH}_3)_2$ ] ppm.  $^{13}\text{C-NMR}$  (400 MHz,  $\text{DMSO-d}_6$ ):  $\delta = 186.58$  (CO), 154.31 ( $\text{CH}_{\text{bpy}}$ ), 145.88 ( $\text{C}_{\text{bpy}}$ ), 137.63 ( $\text{C}_{\text{L2}}$ ), 131.36 ( $\text{C}_{\text{L2}}$ ), 130.70 ( $\text{C}_{\text{L2}}$ ), 129.28 ( $\text{C}_{\text{L2}}$ ), 127.36 ( $\text{C}_{\text{L2}}$ ), 126.56 ( $\text{C}_{\text{L2}}$ ), 126.31 ( $\text{C}_{\text{L2}}$ ), 123.50 ( $\text{CH}_{\text{bpy}}$ ), 114.02 ( $\text{C}_{\text{L2}}$ ), 102.35 ( $\text{C}_{\text{cymene}}$ ), 98.98 ( $\text{C}_{\text{cymene}}$ ), 84.11 ( $\text{CH}_{\text{cymene}}$ ), 82.19 ( $\text{CH}_{\text{cymene}}$ ), 30.90 ( $\text{ArCH}_3$ ), 27.75 (L- $\text{CH}_3$ ), 22.47 [ $\text{CH}(\text{CH}_3)_2$ ], 17.33 [ $\text{CH}(\text{CH}_3)_2$ ] ppm.

**5:** Yield 60 mg, (82%). FT-IR spectrum (KBr,  $\nu$ ,  $\text{cm}^{-1}$ ):  $\nu = 3643$  (w), 2969 (w), 2363 (w), 1609 (s), 1576 (s), 1495 (w), 14210 (m), 1347 (m), 1307 (m), 1091 (m), 1044 (m), 1010 (m), 836 (s), 735 (w), 634 (w), 554 (m), 446 (w)  $\text{cm}^{-1}$ .  $^1\text{H-NMR}$  (400 MHz,  $\text{DMSO-d}_6$ ):  $\delta = 8.54$  (d,  $^3J_{\text{H,H}} = 4$  Hz, 8 H,  $\text{H}_{\text{bpd}}$ ), 8.09 (d,  $^3J_{\text{H,H}} = 8$  Hz, 16 H,  $\text{H}_{\text{bpd}}$ ), 8.03 (d,  $^3J_{\text{H,H}} = 8$  Hz, 8 H,  $\text{H}_{\text{bpd}}$ ), 7.69 (s, 4 H,  $\text{H}_{\text{Ar}}$ ), 7.41 (s, 4 H,  $\text{H}_{\text{Ar}}$ ), 7.25 (s, 4 H,  $\text{H}_{\text{Ar}}$ ), 6.31 (s, 4 H,  $\text{H}_{\text{Ar}}$ ), 6.00 (d,  $^3J_{\text{H,H}} = 8$  Hz, 8 H,  $\text{H}_{\text{cymene}}$ ), 5.77 (d,  $^3J_{\text{H,H}} = 4$  Hz, 8 H,  $\text{H}_{\text{cymene}}$ ), 2.14 [s, 12H,  $\text{ArCH}_3$ ], 1.74 (s, 24 H, L- $\text{CH}_3$ ), 1.36 [d,  $^3J_{\text{H,H}} = 4$  Hz, 24H,

CH(CH<sub>3</sub>)<sub>2</sub>] ppm. <sup>13</sup>C-NMR (400 MHz, DMSO-d<sub>6</sub>): δ = 186.51 (CO), 152.92 (CH<sub>bpd</sub>), 149.30 (C<sub>bpd</sub>), 141.21 (C<sub>bpd</sub>), 138.96 (C<sub>L2</sub>), 138.34 (C<sub>bpd</sub>), 135.03 (C<sub>L2</sub>), 132.19 (C<sub>L2</sub>), 128.36 (CH<sub>bpd</sub>), 128.21 (CH<sub>bpd</sub>), 127.33 (C<sub>L2</sub>), 123.18 (CH<sub>bpd</sub>), 113.69 (C<sub>L2</sub>), 102.08 (C<sub>cymene</sub>), 99.11 (C<sub>cymene</sub>), 84.51 (CH<sub>cymene</sub>), 82.04 (CH<sub>cymene</sub>), 30.81 (ArCH<sub>3</sub>), 28.14 (L-CH<sub>3</sub>), 22.42 [CH(CH<sub>3</sub>)<sub>2</sub>], 17.26 [CH(CH<sub>3</sub>)<sub>2</sub>] ppm.

Metallarectangle with L<sub>2</sub> and L<sub>b</sub>: Yield 63 mg (80%). <sup>1</sup>H-NMR (400 MHz, DMSO-d<sub>6</sub>): δ = 8.57 (d, <sup>3</sup>J<sub>H,H</sub> = 4 Hz, 8 H, H<sub>bpb</sub>), 8.19 (s, 8 H, H<sub>bpb</sub>), 8.15 (d, <sup>3</sup>J<sub>H,H</sub> = 8 Hz, 8 H, H<sub>bpb</sub>), 7.71 (s, 4 H, H<sub>Ar</sub>), 7.43 (s, 4 H, H<sub>Ar</sub>), 7.25 (s, 4 H, H<sub>Ar</sub>), 6.46 (s, 4 H, H<sub>Ar</sub>), 5.99 (d, <sup>3</sup>J<sub>H,H</sub> = 4 Hz, 8 H, H<sub>cymene</sub>), 5.76 (d, <sup>3</sup>J<sub>H,H</sub> = 4 Hz, 8 H, H<sub>cymene</sub>), 2.10 [s, 12H, ArCH<sub>3</sub>], 1.75 (s, 24 H, L-CH<sub>3</sub>), 1.35 [d, <sup>3</sup>J<sub>H,H</sub> = 4 Hz, 24H, CH(CH<sub>3</sub>)<sub>2</sub>] ppm.

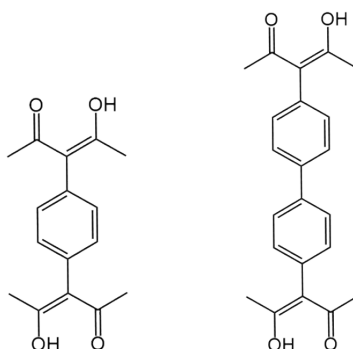


Figure S1. Structure of H<sub>2</sub>L<sub>1</sub> and H<sub>2</sub>L<sub>2</sub>.

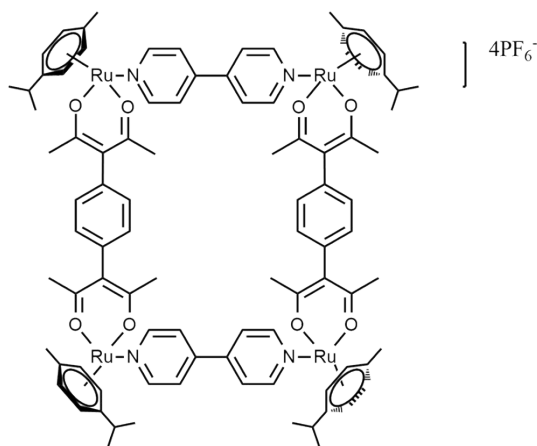


Figure S2. Structure of metallarectangle **1**.

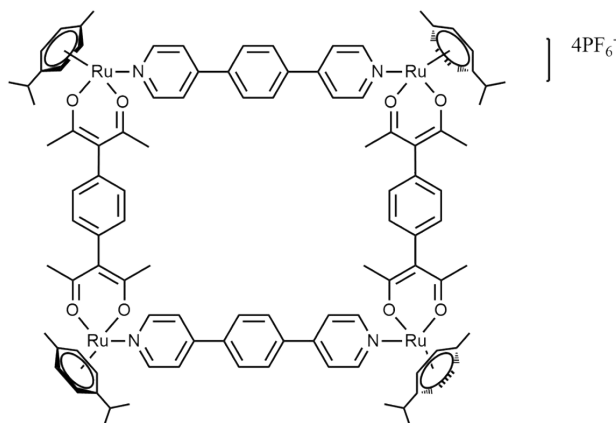


Figure S3. Structure of metallarectangle **2**.

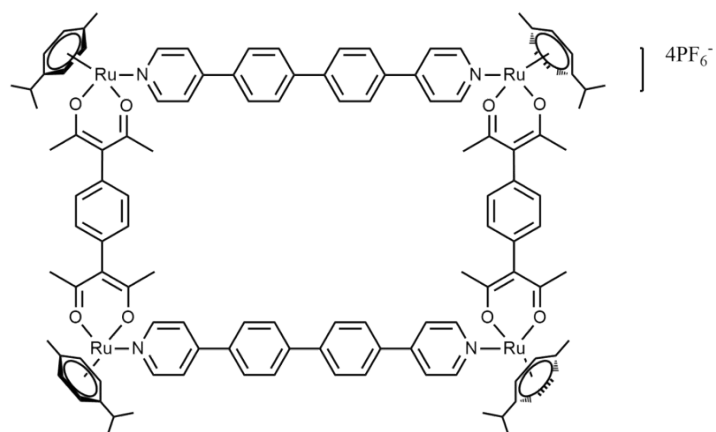


Figure S4. Structure of metallarectangle **3**.

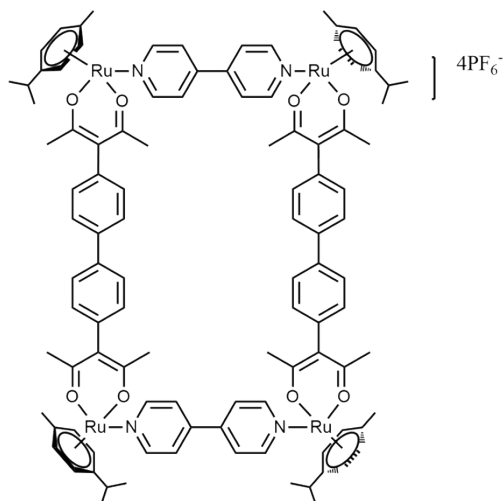


Figure S5. Structure of metallarectangle **4**.

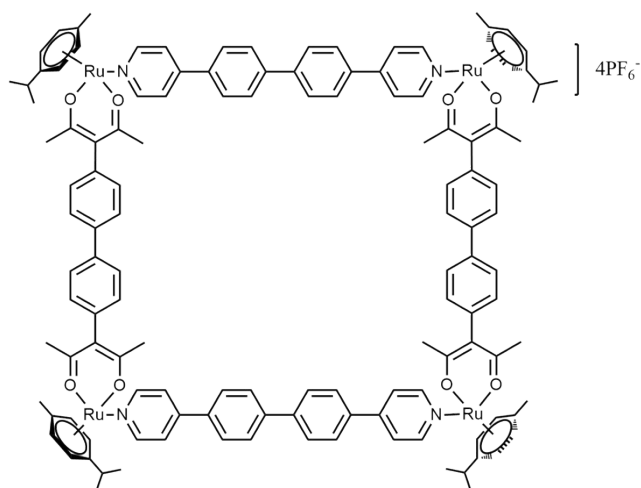


Figure S6. Structure of metallarectangle **5**.

### 3. Single-Crystal Structure Determination

X-ray Crystallography Details. Single crystals of metallarectangle **4** suitable for X-ray diffraction study were obtained at low temperature. X-ray intensity data of data of **4** was collected at 296 K on a Bruker APEXII DUO (APEX II DUO) system. In these data, the disordered solvent molecules which could not be restrained properly were removed using the SQUEEZE route.

#### 4. X-Ray crystal structure parameters of metallarectangle **4**

Table S1. Crystal data and structure refinement for metallarectangle **4**

Empirical formula	C <sub>104</sub> H <sub>112</sub> N <sub>4</sub> O <sub>8</sub> Ru <sub>4</sub>
Formula weight	1950.25
Temperature	296(2)K
Wavelength	0.71073Å
Crystal system	triclinic
Space group	P-1
Unit cell dimensions	a = 10.0358(5) Å, α = 76.380(2)° b = 16.7175(8) Å, β = 79.745(2)° c = 19.5909(10) Å, γ = 78.049(2)°
Volume	3096.1(3) Å <sup>3</sup>
Z	1
Density (calculated)	1.046 Mg/m <sup>3</sup>
Absorption coefficient	0.522 mm <sup>-1</sup>
F(000)	1004.0
Theta range for data collection	2.158 to 52.746
Index ranges	-12<=h<=12, -20<=k<=20, -24<=l<=24
Reflections collected	33650
Independent reflections	12639 [R(int) = 0.0371, R(sigma) = 0.0574]
Completeness to theta = 25.242°	99.7 %
Absorption correction	Semi-empirical from equivalents
Refinement method	Full-matrix least-squares on F <sup>2</sup>
Data / restraints / parameters	12639 / 43 / 541
Goodness-of-fit on F <sup>2</sup>	1.018
Final R indices [I>2sigma(I)]	R <sub>1</sub> = 0.0562, wR <sub>2</sub> = 0.1495
R indices (all data)	R <sub>1</sub> = 0.0818, wR <sub>2</sub> = 0.1603
Largest diff. peak and hole	1.52 and -1.04 e.Å <sup>-3</sup>

#### 5. <sup>1</sup>H NMR spectra of 1-5

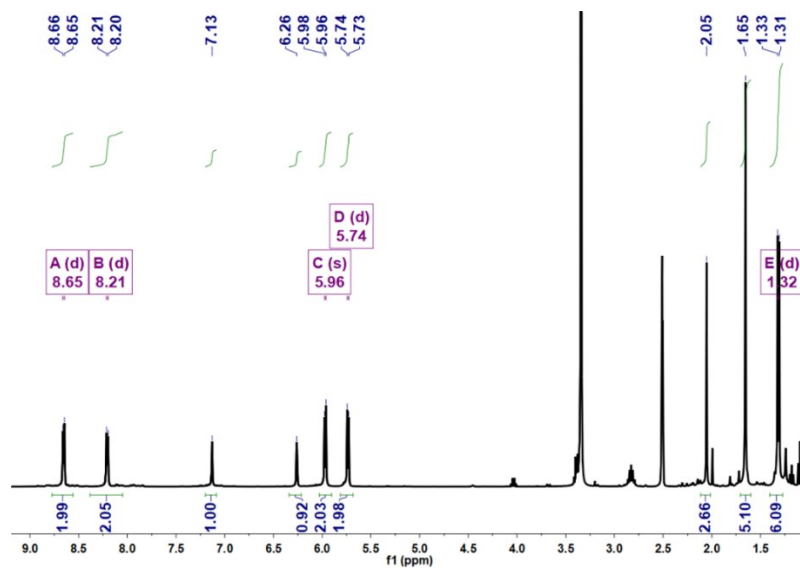


Figure S7.  $^1\text{H}$  NMR spectra (400 MHz,  $\text{DMSO-d}_6$ , 298 K) of metallarectangle 1.

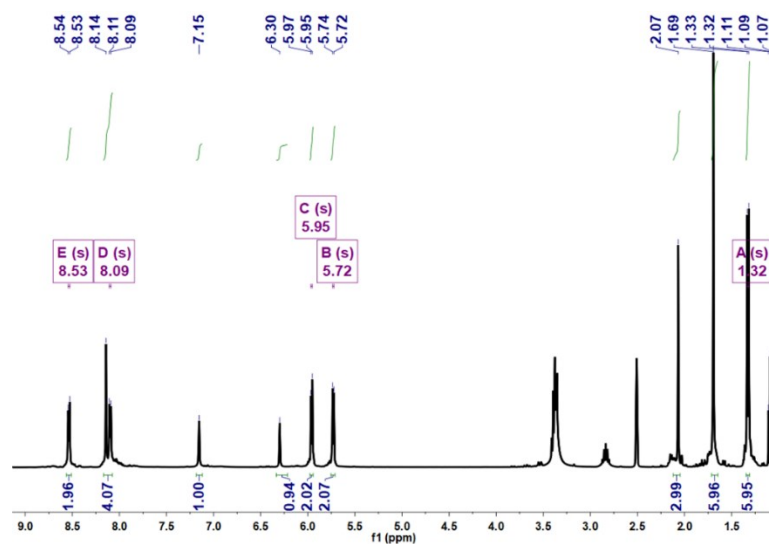


Figure S8.  $^1\text{H}$  NMR spectra (400 MHz,  $\text{DMSO-d}_6$ , 298 K) of metallarectangle 2.

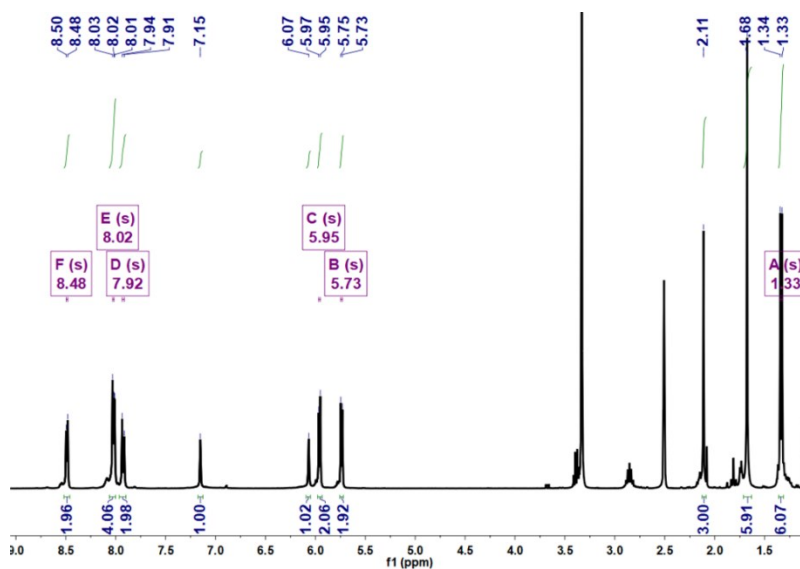


Figure S9.  $^1\text{H}$  NMR spectra (400 MHz,  $\text{DMSO-d}_6$ , 298 K) of metallarectangle **3**.

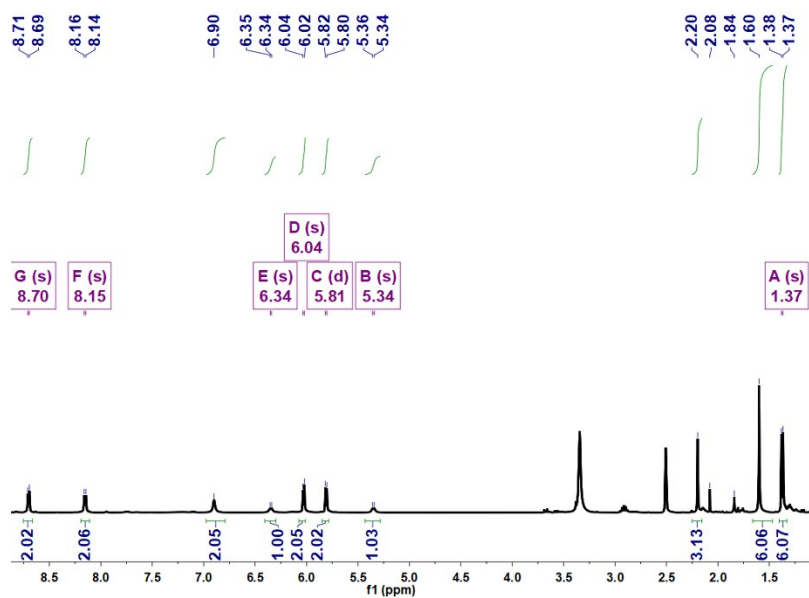
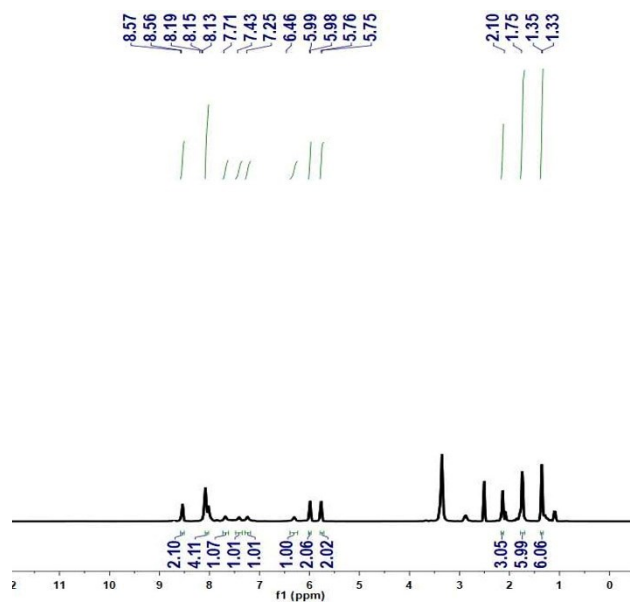


Figure S10.  $^1\text{H}$  NMR spectra (400 MHz,  $\text{DMSO-d}_6$ , 298 K) of metallarectangle **4**.



$^1\text{H}$  NMR spectra (400 MHz,  $\text{DMSO-d}_6$ , 298 K) of metallarectangle synthesized from  $\text{L}_2$  and  $\text{L}_b$ .

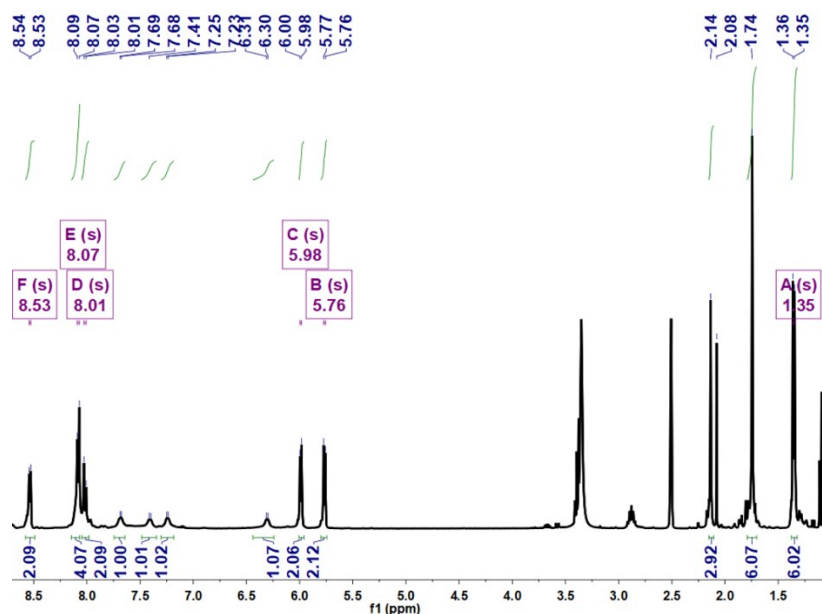


Figure S11.  $^1\text{H}$  NMR spectra (400 MHz,  $\text{DMSO-d}_6$ , 298 K) of metallarectangle **5**.

## 6. ESI-MS spectra of 1-5

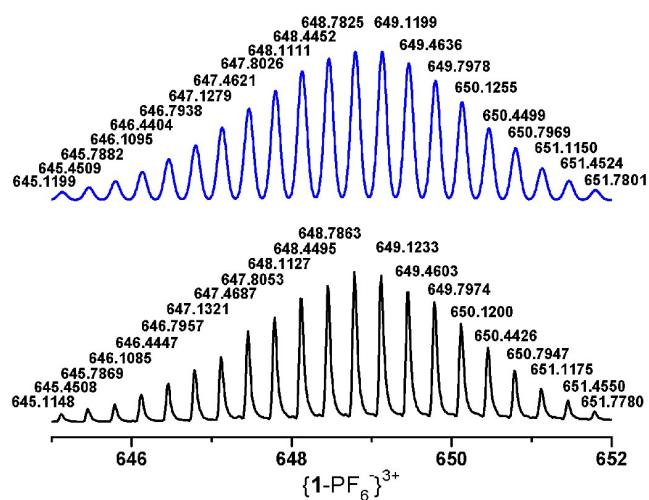


Figure S12. Experimental (below, black) and calculated (above, blue) ESI-MS spectra (3+) of metallarectangle **1**.



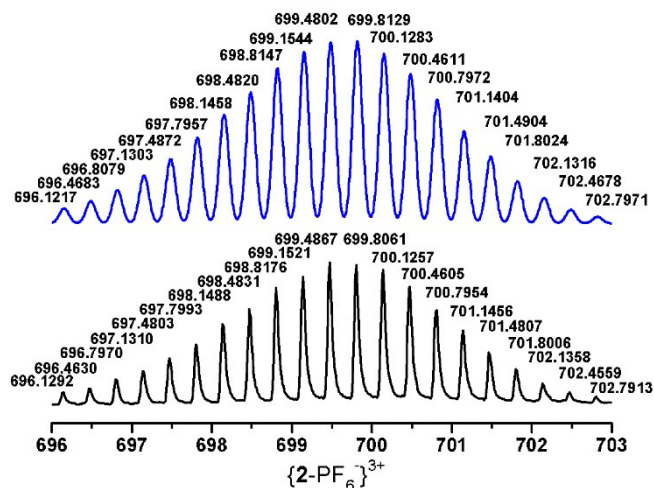


Figure S13. Experimental below, black) and calculated (above, blue) ESI-MS spectra (3+) of metallarectangle 2.

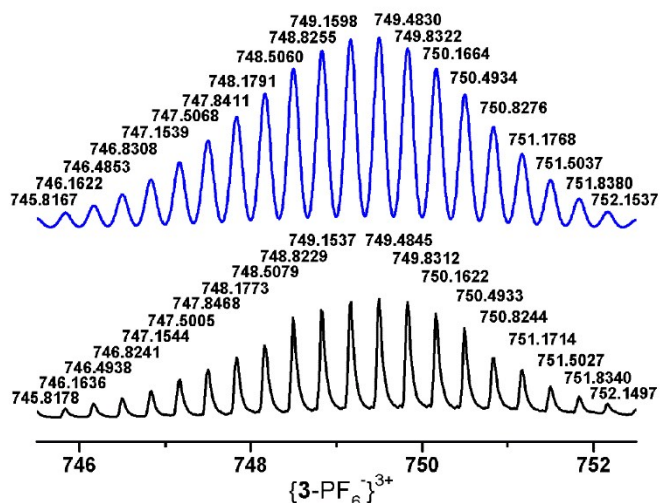


Figure S14. Experimental below, black) and calculated (above, blue) ESI-MS spectra (3+) of metallarectangle 3.

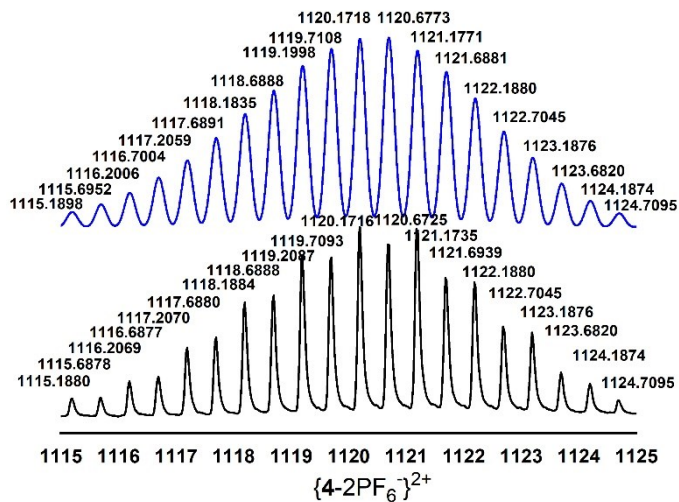


Figure S15. Experimental below, black) and calculated (above, blue) ESI-MS spectra (2+) of metallarectangle 4.

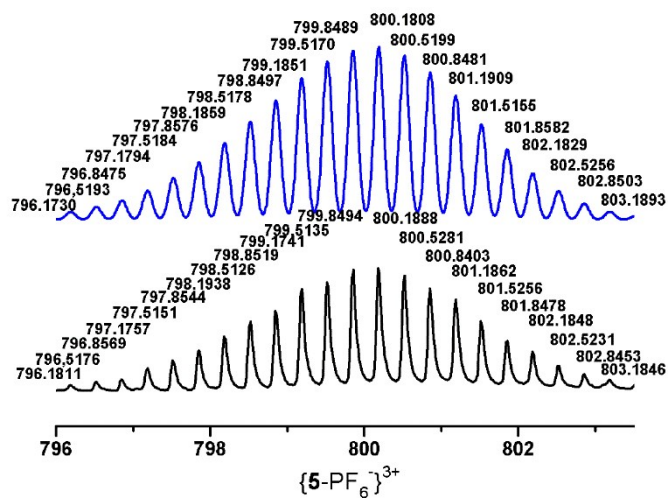


Figure S16. Experimental below, black) and calculated (above, blue) ESI-MS spectra (3+) of metallarectangle 5.

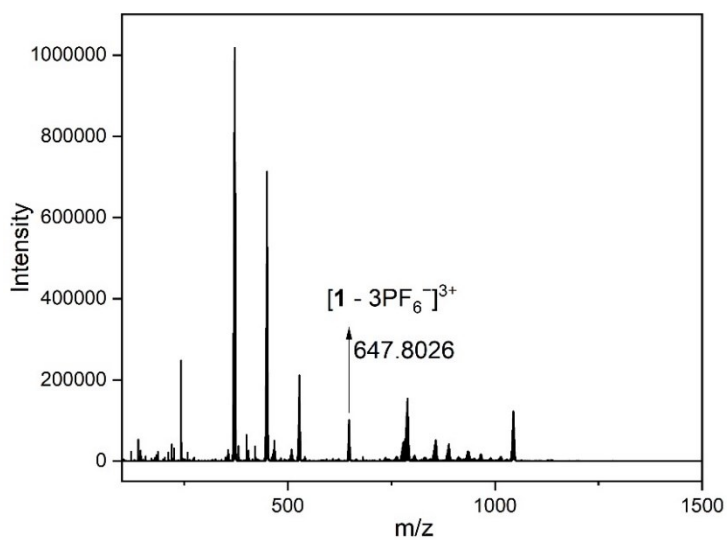


Figure S17. The ESI-MS spectra of metallarectangle 1.

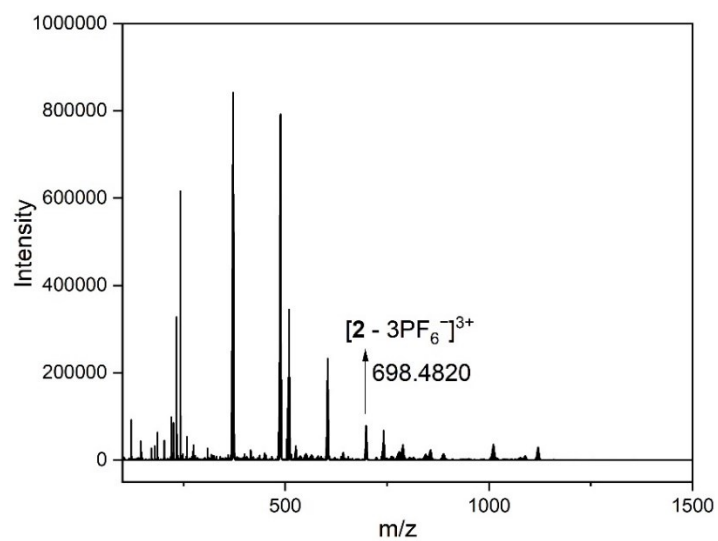


Figure S18. The ESI-MS spectra of metallarectangle **2**.

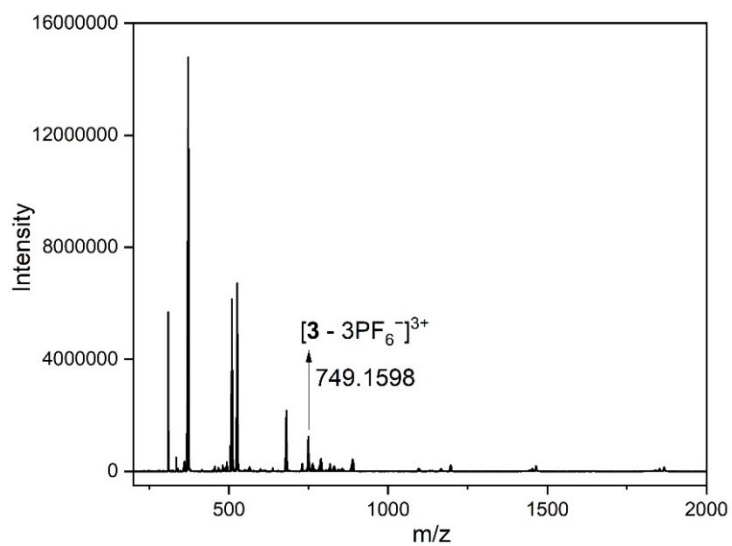


Figure S19. The ESI-MS spectra of metallarectangle **3**.

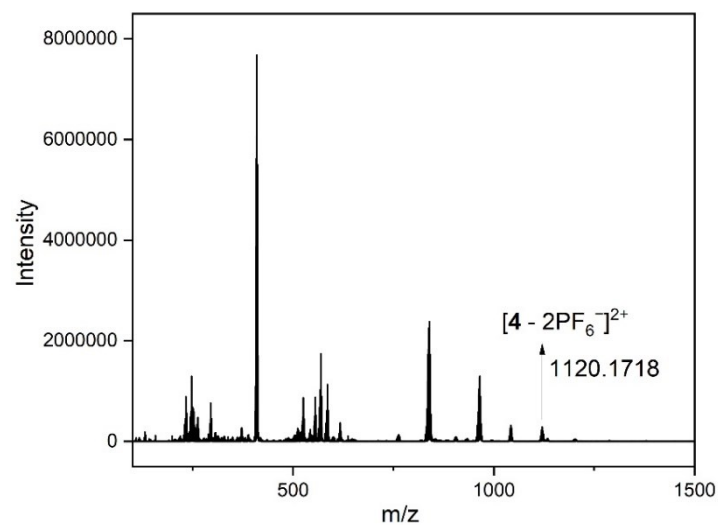


Figure S20. The ESI-MS spectra of metallarectangle 4.

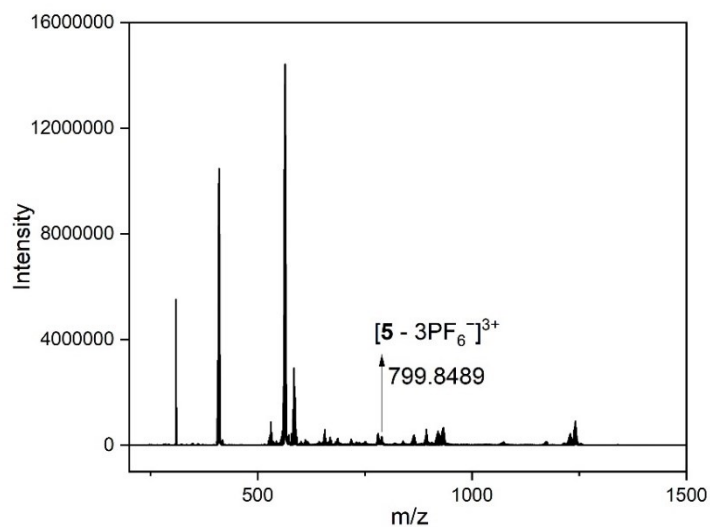


Figure S21. The ESI-MS spectra of metallarectangle 5.

## 7. IR spectra of 1-5

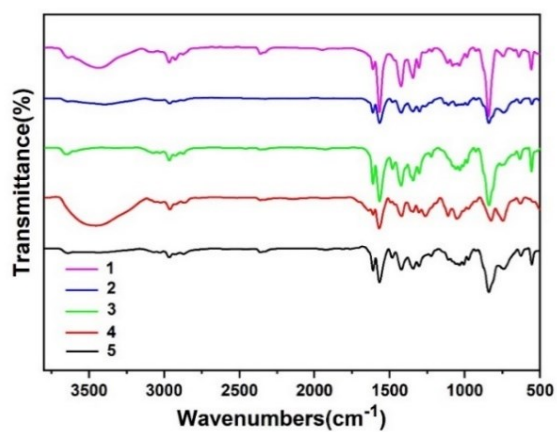


Figure S22. IR spectra of metallarectangle 1-5.

## 8. Absorption spectra

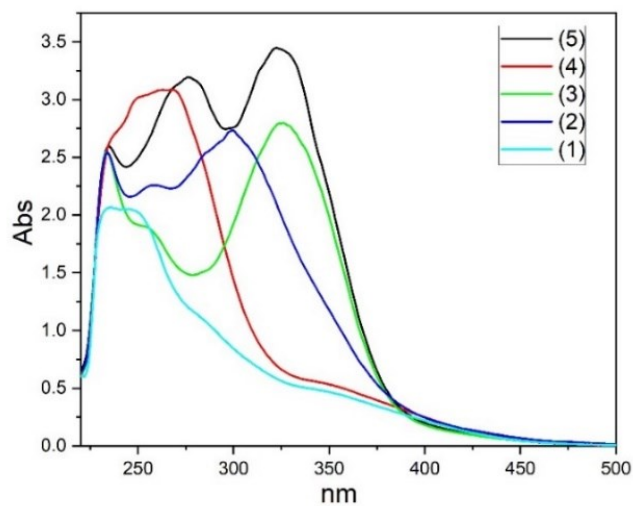


Figure S23. Absorption spectra of metallarectangle **1-5** in  $\text{CH}_2\text{Cl}_2$  ( $c = 2.0 \times 10^{-5}$  M).

## 9. The photoluminescence (PL) emission spectra

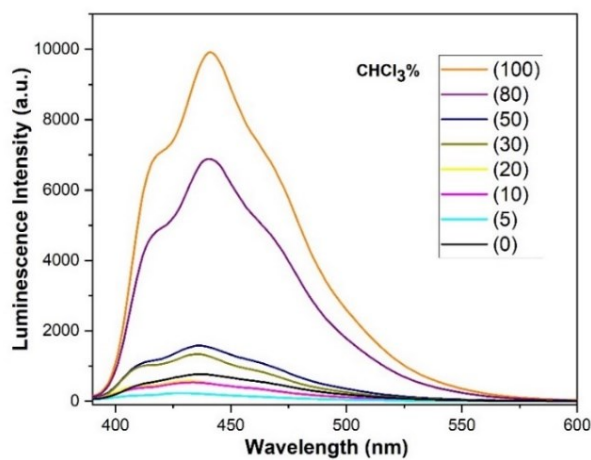


Figure S24. Emission spectra of metallarectangle **1** versus  $\text{CHCl}_3$  fraction in  $\text{CHCl}_3/\text{acetone}$  mixtures ( $c = 2.0 \times 10^{-5}$  M,  $\lambda_{\text{exc}} = 375$  nm).

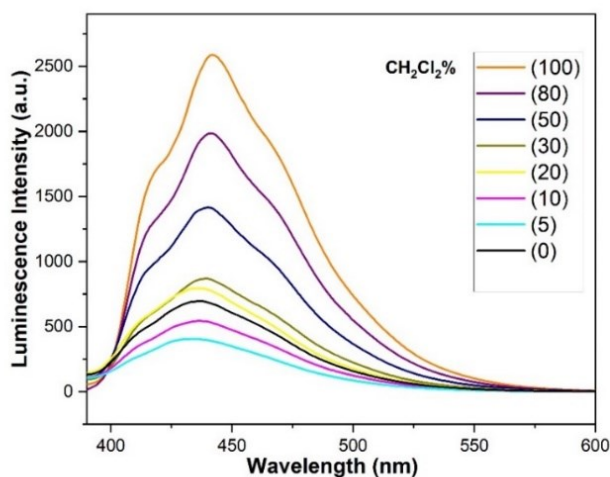


Figure S25. Emission spectra of metallarectangle **1** versus  $\text{CH}_2\text{Cl}_2$  fraction in  $\text{CH}_2\text{Cl}_2/\text{acetone}$  mixtures ( $c = 2.0 \times 10^{-5}$  M,  $\lambda_{\text{exc}} = 375$  nm).

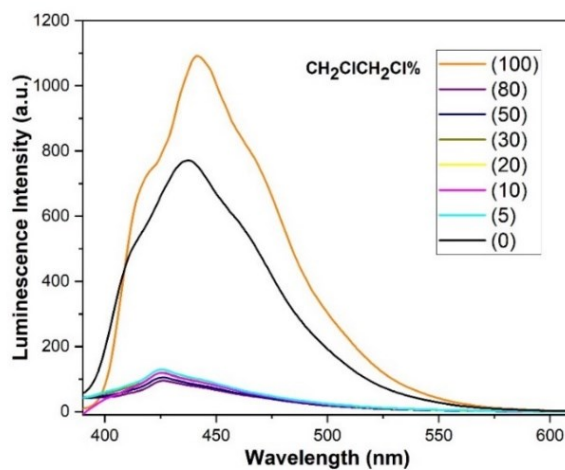


Figure S26. Emission spectra of metallarectangle **1** versus CH<sub>2</sub>ClCH<sub>2</sub>Cl fraction in CH<sub>2</sub>ClCH<sub>2</sub>Cl/acetone mixtures ( $c = 2.0 \times 10^{-5}$  M,  $\lambda_{\text{ex}} = 375$  nm).

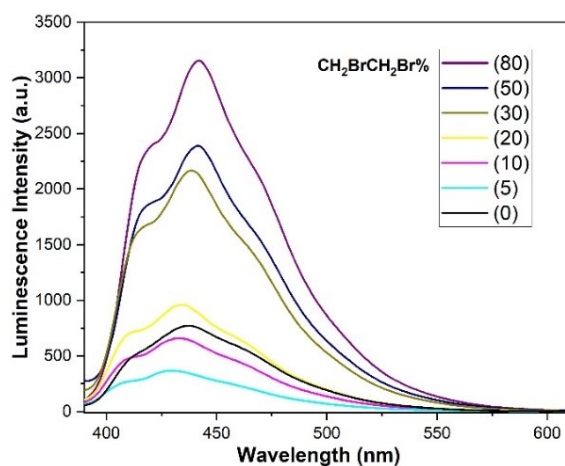


Figure S27. Emission spectra of metallarectangle **1** versus CH<sub>2</sub>BrCH<sub>2</sub>Br fraction in CH<sub>2</sub>BrCH<sub>2</sub>Br/acetone mixtures ( $c = 2.0 \times 10^{-5}$  M,  $\lambda_{\text{ex}} = 375$  nm).

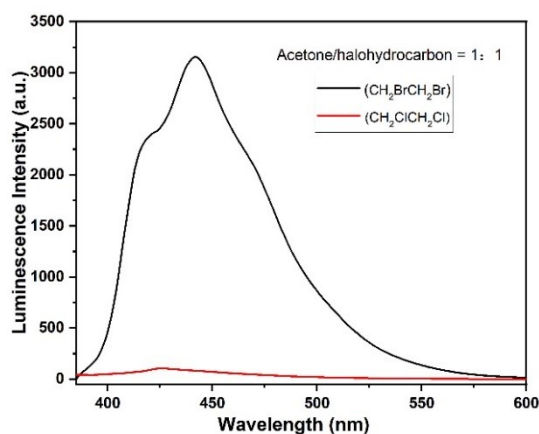


Figure S28. Emission spectra of metallarectangle **1** in acetone/haloalkane = 1:1 mixed solution ( $c = 2.0 \times 10^{-5}$  M,  $\lambda_{\text{ex}} = 375$  nm).

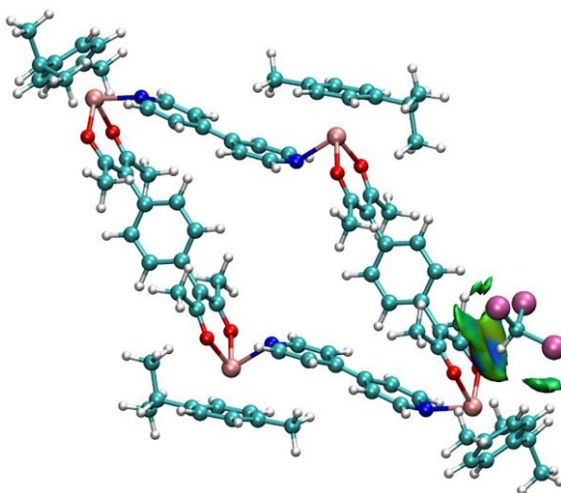


Figure S29. Independent Gradient Method (IGM) analysis the interaction of complex **1** and CHCl<sub>3</sub>.

Color code: pink-Ru; mauve-chlorine; blue-nitrogen; red-oxygen; cyan-carbon; white-hydrogen.

To evaluate the noncovalent interactions between metallarectangles and haloalkane molecules, the Independent Gradient Method (IGM)<sup>2</sup> is performed by Multiwfn program.<sup>3</sup> The strong attractive/repulsive interaction and VDW (Van der Waals) interaction are shown in blue/red and green, respectively.

## 10. References

S1 M. Rancan, A. Dolmella, R. Seraglia, S. Orlandi, S. Quici, L. Sorace, D. Gatteschi, L. Armelao, *Inorg. Chem.*, 2012, 51, 5409-5416.

S2 C. Lefebvre, G. Rubez, H. Khartabil, J. C. Boisson, J. Contreras-Garcia, E. Henon, Accurately extracting the signature of intermolecular interactions present in the NCI plot of the reduced density gradient versus electron density, *Phys. Chem. Chem. Phys.*, 2017, 19, 17928-17936.

S3 T. Lu, F. Chen, Multiwfn: a multifunctional wavefunction analyzer, *J. Comput. Chem.*, 2012, 33, 580-592.